Pharmaceutical Sciences and Drug Design
ISSN: 3062-4428
2025, Volume 5, Page No: 167-180

Available online at: www.galaxypub.co/page/journals

Galaxy Publication

Inhibition of NF-κB and ERK Signaling by Pristimerin Mitigates Osteoclast Formation and OVX-Induced Bone Loss

Amanda Brooks[1]*, Ellie Watson[1]

[1]Department of Pharmacognosy, Faculty of Pharmacy, University of British Columbia, Vancouver, Canada.

***E-mail** ✉ amanda.brooks.ca@outlook.com

Received: 08 April 2025; **Revised:** 16 August 2025; **Accepted:** 21 August 2025

ABSTRACT

Osteoporosis is a bone disorder marked by reduced bone density and increased fracture risk, primarily due to enhanced formation or activity of bone-resorbing osteoclasts. Although current anti-resorptive therapies can effectively reduce osteoclast-mediated bone loss, their long-term use is often limited by adverse effects. Pristimerin (PRI), a naturally occurring quinone-methide triterpenoid, has been reported to possess anti-inflammatory and anti-cancer properties through modulation of signaling pathways, including NF-κB and MAPK. The anti-osteoclastic and bone-resorptive effects of PRI were examined in vitro using bone marrow-derived macrophages. Additionally, an ovariectomized (OVX) mouse model was employed to evaluate the protective effects of PRI against bone loss in vivo. PRI inhibited early activation of NF-κB and ERK MAPK signaling, thereby suppressing downstream targets c-Fos and NFATc1 and preventing osteoclast maturation. In the OVX model, PRI effectively mitigated bone loss by reducing osteoclast formation and resorptive activity. These findings suggest that PRI holds promise as a therapeutic agent for osteoclast-driven bone diseases such as osteoporosis by targeting key signaling pathways involved in osteoclast differentiation and function.

Keywords: Osteoclast, Pristimerin, Osteoporosis, ERK, NF-κB

How to Cite This Article: Brooks A, Watson E. Inhibition of NF-κB and ERK Signaling by Pristimerin Mitigates Osteoclast Formation and OVX-Induced Bone Loss. Pharm Sci Drug Des. 2025;5:167-80. https://doi.org/10.51847/euUWdFZfyK

Introduction

Bone tissue undergoes continuous remodeling to preserve structural integrity, a process maintained by the coordinated actions of osteoclasts, which resorb bone, and osteoblasts, which form bone [1]. Disruption of this balance, particularly due to excessive osteoclast formation or activity, is a central cause of osteolytic diseases such as postmenopausal osteoporosis [2]. Overactive osteoclast-mediated bone resorption leads to reduced bone mass, decreased mineral density, deterioration of bone microarchitecture, and heightened fracture risk [3]. Osteoporosis-related fractures remain a major public health concern worldwide, contributing to morbidity, mortality, and elevated healthcare expenditures. Current anti-resorptive treatments can mitigate bone loss effectively, but long-term use is often limited by adverse effects including ocular, renal, gastrointestinal toxicity, atypical fractures, and osteonecrosis of the jaw [4, 5]. This has driven interest in novel therapeutic strategies that target the molecular pathways regulating osteoclastogenesis.

Osteoclasts develop from monocyte/macrophage lineage precursors under the influence of two critical cytokines: macrophage colony-stimulating factor (M-CSF) and receptor activator of nuclear factor-κB ligand (RANKL) [6, 7]. M-CSF promotes precursor proliferation and survival while enhancing RANK receptor expression, allowing osteoclast precursors to respond to RANKL, a TNF-family protein secreted or presented by osteoblasts and stromal cells [8]. Binding of RANKL to RANK triggers downstream signaling via TRAF proteins and other adaptor molecules, leading to activation of NF-κB and MAPK pathways. This early signaling cascade induces nuclear factor of activated T cells 1 (NFATc1), the master transcription factor driving osteoclast differentiation

[9, 10]. NFATc1 then orchestrates the expression of genes critical for osteoclast fusion (e.g., Dc-stamp) and bone-resorbing enzymes (e.g., Trap/Acp5, Cathepsin K, Mmp-9) [11].

Pristimerin (PRI) is a naturally occurring quinone-methide triterpenoid found in plants of the Celastraceae and Hippocrateaceae families. PRI exhibits multiple pharmacological activities, including anti-inflammatory [12] and anticancer effects [13], mediated via pathways such as Akt/NF-κB and ROS/MAPK [14]. Moreover, PRI has demonstrated protective effects against arthritis-induced bone and cartilage damage by modulating RANKL and inflammatory cytokine expression [15]. Based on these findings, we hypothesized that PRI could inhibit RANKL-induced osteoclast formation and resorptive function. In this study, we employed in vitro cellular and biochemical assays to investigate the effects of PRI on osteoclast differentiation and function, and further evaluated its therapeutic potential in vivo using a murine ovariectomy (OVX) model that recapitulates postmenopausal osteoporosis [16].

Materials and Methods

Reagents and cell culture

Pristimerin (≥98% purity) was purchased from Chengdu Biopurify Phytochemicals Ltd (Chengdu, Sichuan, China) and prepared as a 20 mM stock solution in dimethyl sulfoxide (DMSO), then diluted in culture medium for experiments. α-MEM medium supplemented with 10% fetal bovine serum (FBS) and 1% penicillin/streptomycin was used for cell culture (Thermo Fisher Scientific, Scoresby, Victoria, Australia). Recombinant murine RANKL and M-CSF were obtained from R&D Systems (Minneapolis, MN, USA). Primary antibodies targeting p38, phospho-p38, JNK, phospho-JNK, ERK, phospho-ERK, NF-κB p65, phospho-NF-κB p65, β-actin, and IκBα were purchased from Cell Signaling Technology (Danvers, MA, USA). NFATc1 antibodies were sourced from Santa Cruz Biotechnology (Dallas, TX, USA), and c-Fos antibodies from Abcam (Cambridge, UK). Cell counting kit-8 (CCK-8) was obtained from MedChemExpress LLC (Monmouth Junction, NJ, USA). Rhodamine-conjugated phalloidin and DAPI were purchased from Molecular Probes (Eugene, OR, USA) and Sigma-Aldrich (St. Louis, MO, USA), respectively.

Cell culture and osteoclast differentiation

Bone marrow macrophages (BMMs) were harvested from the femurs and tibias of six-week-old C57BL/6 mice by flushing the marrow cavity. Cells were maintained in α-MEM supplemented with 30 ng/mL M-CSF at 37°C in a humidified incubator containing 5% CO_2. Media were refreshed every two days to remove non-adherent cells, and after four days, adherent cells were considered BMMs suitable for downstream experiments [1].

For osteoclastogenesis, BMMs were plated at 8×10^3 cells per well in 96-well plates and allowed to attach overnight. The next day, cells were treated with 50 ng/mL RANKL in the absence or presence of varying concentrations of pristimerin (PRI; 0.3125, 0.625, or 1.25 μM) for six days. To determine the differentiation stage at which PRI exerted its effects, cells were exposed to 1.25 μM PRI during early (days 1–3), mid (days 3–5), or late (days 5–6) osteoclastogenesis. Cells treated with RANKL alone served as positive controls. Culture media containing RANKL and PRI were replaced every two days. At the end of the experiment, cells were fixed with 4% paraformaldehyde for 30 minutes and stained for tartrate-resistant acid phosphatase (TRAP). TRAP-positive cells with three or more nuclei were considered mature osteoclasts and quantified under a phase-contrast microscope [2].

Cell viability assay

BMM viability under PRI exposure was measured using the CCK-8 assay. Cells were plated at 8×10^3 cells/well in 96-well plates and incubated with 0.3125, 0.625, or 1.25 μM PRI for 48 hours. After incubation, 10 μL of CCK-8 solution was added to each well and incubated for an additional two hours. Absorbance at 450 nm was measured using a TriStar2 LB 942 Multimode Microplate Reader (Berthold Technologies GmbH & Co.KG, Germany) [3].

Podosomal actin belt staining

To evaluate the effects of PRI on the osteoclast cytoskeleton, mature osteoclasts were generated as described above with PRI at concentrations of 0, 0.3125, 0.625, or 1.25 μM. After six days, cells were fixed with 4% PFA for 15 minutes, permeabilized with 0.1% Triton X-100 for five minutes, and washed with PBS. Cells were blocked with 3% BSA in PBS for 30 minutes, then stained with Rhodamine-conjugated phalloidin (0.2% BSA-PBS) for

one hour in the dark. Nuclei were counterstained with DAPI for five minutes. Fluorescence images were acquired using a Cytation 5 imaging system and analyzed using Gen5 software (BioTek Instruments Inc., USA) [4].

Bone resorption assay

To assess osteoclast-mediated bone resorption, BMMs were plated in 6-well plates at 1×10^5 cells/well and cultured with 50 ng/mL RANKL for three days to generate pre-osteoclasts. These cells were detached with trypsin and reseeded in equal numbers onto 96-well plates coated with a hydroxyapatite matrix. Cells were treated with RANKL in combination with PRI (0, 0.3125, 0.625, or 1.25 μM) for an additional three days. Cells were removed using sodium hypochlorite, and resorption pits were visualized under a light microscope. The resorbed areas were quantified using ImageJ software (NIH, USA) [5].

RNA extraction and quantitative PCR (qPCR)

Total RNA was isolated from BMM-derived osteoclasts treated with RANKL, with or without PRI (0.625 or 1.25 μM), using TRIzol reagent (Thermo Fisher Scientific). Complementary DNA (cDNA) was synthesized using the RevertAid First Strand cDNA Synthesis Kit (Thermo Fisher Scientific). Quantitative PCR was performed on a LightCycler® 96 System (Roche) with FastStart Essential DNA Green Master Mix (Roche). The cycling program consisted of an initial denaturation at 95°C for 10 minutes, followed by 35 cycles at 95°C for 10 seconds, 60°C for 15 seconds, and 72°C for 10 seconds. Relative gene expression levels were calculated using the $2^{-}\Delta\Delta Ct$ method and normalized to β-actin. The primer sequences were:

- **Ctsk**: F 5′-AGGCGGCTATATGACCACTG-3′, R 5′-TCTTCAGGGCTTTCTCGTTC-3′
- **Trap/Acp5**: F 5′-ACGGCTACTTGCGGTTTCA-3′, R 5′-TCCTTGGGAGGCTGGTCTT-3′
- **Mmp-9**: F 5′-GAAGGCAAACCCTGTGTGTT-3′, R 5′-AGAGTACTGCTTGCCCAGGA-3′
- **Dc-stamp**: F 5′-TCTGCTGTATCGGCTCATCTC-3′, R 5′-ACTCCTTGGGTTCCTTGCTT-3′
- **β-actin**: F 5′-TCCTCCCTGGAGAAGAGCTA-3′, R 5′-ATCTCCTTCTGCATCCTGTC-3′ [6].

Protein extraction and western blot analysis

To examine the effects of PRI on early RANKL-triggered signaling, BMMs were plated at 1×10^6 cells per well in 6-well plates and allowed to adhere overnight. Cells were serum-starved for three hours, pretreated with 1.25 μM PRI for one hour, and then stimulated with 50 ng/mL RANKL for 5, 10, 20, 30, or 60 minutes. For analysis of later signaling events, BMMs (1×10^5 cells/well) were cultured with RANKL in the presence or absence of 1.25 μM PRI for 1, 3, or 5 days. Unstimulated BMMs served as controls (time 0). Protein extraction was performed using RIPA buffer containing 1% PMSF, 1% protease inhibitor, and 1% phosphatase inhibitor. Lysates were centrifuged at 15,000 rpm for 10 minutes, and supernatants were collected for protein quantification. Equal amounts of protein were resolved by 10–12% SDS-PAGE and transferred to nitrocellulose membranes. Membranes were blocked with 5% skim milk in TBST for one hour at 37°C and incubated overnight at 4°C with specific primary antibodies diluted in 1% skim milk-TBST. Following washes, membranes were probed with corresponding secondary antibodies and visualized using an Odyssey Sa Infrared Imaging System (LI-COR Biosciences, USA). Band intensity was quantified with ImageJ software [1].

Immunofluorescence for NF-κB p65 and NFATc1 nuclear translocation

Nuclear translocation of NF-κB p65 and NFATc1 was assessed using confocal microscopy. For NF-κB p65, BMMs were plated on microscopy dishes overnight, serum-starved for 3 hours, pretreated with or without 1.25 μM PRI for 1 hour, and then stimulated with 50 ng/mL RANKL for 30 minutes. For NFATc1, BMMs were treated with RANKL ± PRI (1.25 μM) for 5 days. Cells were fixed in 4% PFA for 15 minutes, permeabilized with 0.1% Triton X-100 for 5 minutes, and blocked with 3% BSA-PBS for 30 minutes. Primary antibodies against NF-κB p65 (sc-8008 PE; Santa Cruz Biotechnology) or NFATc1 (sc-7294 AF488; Santa Cruz Biotechnology) were incubated overnight at 4°C, followed by secondary antibody staining (Alexa Fluor 552 for NF-κB p65 or Alexa Fluor 488 for NFATc1) for 1 hour in the dark. Nuclei were counterstained with DAPI, and images were captured by confocal microscopy [2].

OVX-Induced osteoporosis model

To evaluate the in vivo protective effect of PRI against postmenopausal bone loss, a bilateral ovariectomy (OVX) model was performed in 12-week-old female C57BL/6 mice. All procedures were approved by the Ethics

Committee of Guangxi Medical University. Mice were randomly assigned to three groups (n = 8 per group): Sham + saline, OVX + saline, and OVX + PRI (5 mg/kg). Mice were anesthetized with tribromoethanol, ovariectomized, or sham-operated, and received intraperitoneal penicillin to prevent infections. One week post-surgery, PRI or saline was administered intraperitoneally every two days for six weeks. After treatment, mice were euthanized, and tibiae were harvested for micro-CT and histological analyses [3].

Micro-CT imaging and histology

Fixed tibiae (4% PFA, 24 h) were scanned using a Bruker micro-CT system at 70 kV, 142 μA, and a 10 μm isotropic voxel size. Three-dimensional reconstructions and quantitative analysis of trabecular bone parameters—BMD, connectivity density (Conn.D), trabecular number (Tb.N), trabecular separation (Tb.Sp), trabecular thickness (Tb.Th), and BV/TV—were performed using CTAn software. For histology, bones were decalcified in 10% EDTA at 4°C for one week, embedded in paraffin, and sectioned at 5 μm. Sections were stained with H&E and TRAP, and osteoclast numbers were quantified in a blinded manner [4].

Statistical analysis

All data are presented as mean ± SD. Experiments were independently repeated at least three times. Statistical comparisons were made using Student's t-test or one-way ANOVA with GraphPad Prism 7.0. P-values < 0.05 were considered statistically significant [5].

PRI suppresses RANKL-driven osteoclast formation in vitro

To determine whether PRI influences osteoclastogenesis, we first tested its cytotoxicity on BMMs using the CCK-8 assay. As depicted in **Figure 1b**, PRI did not exhibit noticeable toxicity at concentrations up to 1.25 μM after 48 hours of exposure. Based on the typical timeframe of 5–6 days required for RANKL to induce osteoclast differentiation, three concentrations of PRI (0.3125, 0.625, and 1.25 μM) were selected for further studies. Subsequent experiments assessed the effects of PRI on RANKL-induced osteoclast development. BMMs treated with RANKL alone formed large, well-spread, TRAP-positive multinucleated osteoclasts **(Figure 1c)**. In contrast, PRI treatment caused a clear, dose-dependent reduction in the formation of multinucleated osteoclasts, with the highest dose (1.25 μM) primarily yielding TRAP-positive mononuclear cells **(Figures 1c and 1d)**.

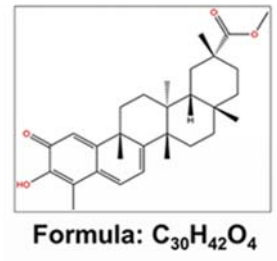

a)

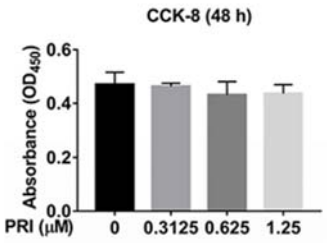

b)

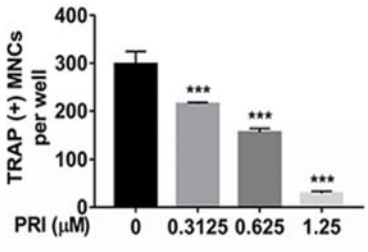

d)

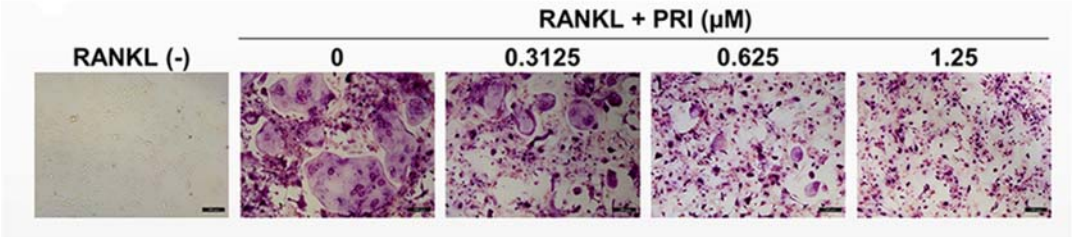

c)

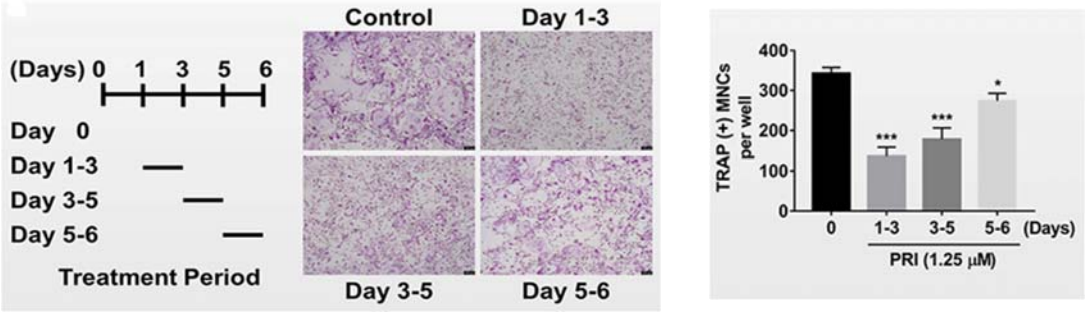

e) f)

Figure 1. PRI Suppresses RANKL-Induced Osteoclast Differentiation In Vitro
(a) Chemical structure and molecular formula of Pristimerin (PRI).
(b) Assessment of cytotoxicity of various PRI concentrations on bone marrow macrophages (BMMs) after 48 hours using the CCK-8 assay.
(c) Representative TRAP-stained phase-contrast images showing the dose-dependent inhibitory effect of PRI on RANKL-induced osteoclast formation over 6 days (50 ng/mL RANKL; scale bar = 200 μm).
(d) Quantification of TRAP-positive multinucleated osteoclasts (≥3 nuclei).
(e) Representative TRAP-stained images illustrating the time-dependent inhibitory effect of PRI on osteoclast formation. BMMs were treated with 1.25 μM PRI at different stages of RANKL stimulation (scale bar = 100 μm).
(f) Quantification of TRAP-positive multinucleated osteoclasts (≥3 nuclei) at each treatment stage. Data are presented as mean ± SD from at least three independent experiments; *$p < 0.05$, ***$p < 0.001$ vs. RANKL-only controls. All experiments were performed in triplicate.

To determine the specific stage of osteoclast differentiation affected by PRI, RANKL-stimulated BMMs were exposed to 1.25 μM PRI during defined periods of the 6-day culture **(Figure 1e).** PRI exerted the most pronounced inhibitory effect when applied during the early differentiation stage (days 1–3), markedly reducing TRAP-positive multinucleated osteoclasts compared to RANKL-only controls **(Figures 1e and 1f)**. Treatment during the late stage (days 5–6) produced a modest but significant reduction, while administration during the intermediate stage (days 3–5) yielded an intermediate effect. These findings indicate that PRI primarily suppresses the differentiation and fusion of BMM precursors in response to RANKL stimulation.

PRI attenuates osteoclast resorptive function in vitro

The assembly of podosomal actin belts and mature F-actin rings is essential for osteoclast bone resorption [17]. To investigate the impact of PRI on osteoclast cytoskeletal organization, BMM-derived osteoclasts were treated with varying concentrations of PRI and stained with Rhodamine-conjugated phalloidin. Consistent with its inhibitory effects on osteoclastogenesis, PRI treatment reduced both the formation and size of podosomal actin belts in a dose-dependent manner **(Figure 2a)**. The highest concentration (1.25 μM) largely prevented precursor cell fusion, resulting in predominantly mononuclear cells devoid of actin rings, further confirming the suppression of early osteoclast development.

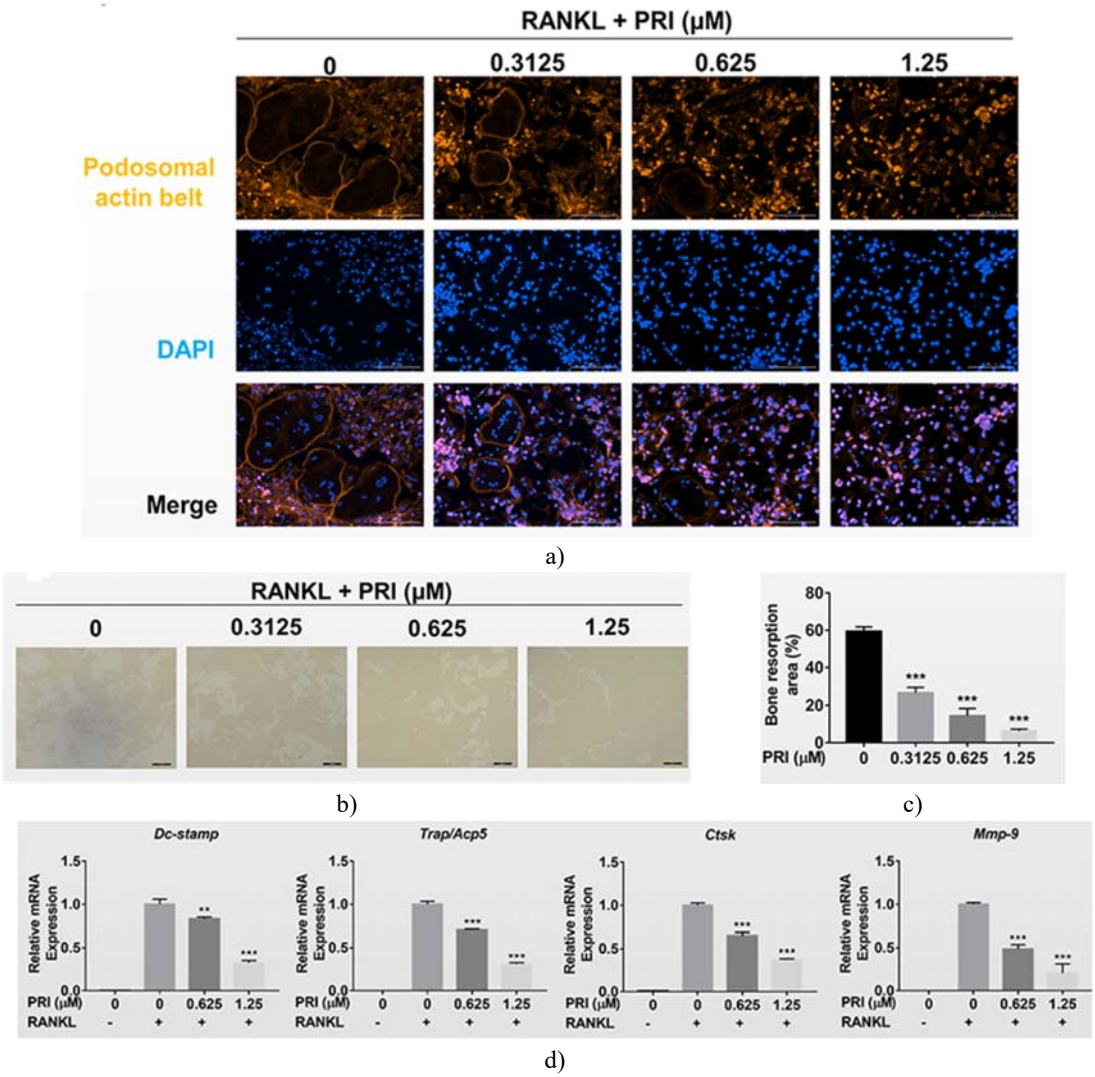

Figure 2. PRI Inhibits Podosomal Actin Belt Formation and Bone Resorption in Mature Osteoclasts In Vitro
(a) Immunofluorescence images showing podosomal actin belts (Rhodamine-phalloidin, red) in BMM-derived osteoclasts treated with 50 ng/mL RANKL in the absence or presence of PRI. Nuclei were counterstained with DAPI (blue).
(b) Representative phase-contrast images demonstrating the effect of PRI on mature osteoclast-mediated bone resorption. Pre-osteoclasts were cultured with RANKL for 3 days, then reseeded onto hydroxyapatite-coated plates and treated with PRI for an additional 3 days (scale bar = 200 μm).
(c) Quantification of bone resorption area relative to total well area, analyzed using ImageJ.
(d) Dose-dependent suppression of osteoclast marker gene expression by PRI. mRNA levels of Dc-stamp, Trap/Acp5, Ctsk, and Mmp-9 were measured by qPCR after 6 days of RANKL stimulation with or without PRI, normalized to β-actin, and presented as fold change relative to RANKL-only controls. Data represent mean ± SD of at least three independent experiments; **p < 0.01, ***p < 0.001 vs RANKL-only control.

PRI suppresses bone resorptive activity of mature osteoclasts

Osteoclasts are uniquely responsible for resorbing mineralized bone matrix. To evaluate whether PRI affects this functional activity, pre-osteoclasts cultured for 3 days were reseeded onto hydroxyapatite-coated plates and treated with various concentrations of PRI for 3 additional days. PRI treatment dose-dependently reduced the resorption area compared to controls **(Figures 2b and 2c)**, demonstrating that PRI not only inhibits osteoclast formation but also diminishes the bone-resorptive function of mature osteoclasts.

PRI inhibits RANKL-induced upregulation of osteoclast-specific genes

Osteoclast differentiation and bone resorption require the induction of genes essential for precursor fusion (Dc-stamp) and proteolytic activity (Ctsk, Trap/Acp5, Mmp-9) **(Figure 2d)**. Consistent with its inhibitory effects on osteoclast formation and resorption, PRI significantly suppressed the RANKL-mediated upregulation of these genes, confirming its dual anti-osteoclastic and anti-resorptive actions.

PRI blocks RANKL-induced activation of NF-κB and ERK pathways

The expression of osteoclast-specific genes is tightly regulated by signaling cascades triggered by RANKL, particularly the NF-κB and MAPK pathways. Activation of these pathways is essential for directing BMM precursors towards osteoclast differentiation. Western blot analyses revealed that RANKL stimulation caused rapid degradation of the NF-κB inhibitory protein IκBα within 5 minutes, persisting up to 30 minutes **(Figures 3a and 3b)**. IκBα degradation exposes the nuclear localization signal of NF-κB p65, allowing its phosphorylation (5–10 minutes) **(Figures 3and 3c)** and nuclear translocation **(Figure 3d)**, where it promotes transcription of target genes [18]. Treatment with 1.25 μM PRI effectively prevented IκBα degradation, p65 phosphorylation, and nuclear translocation, demonstrating that PRI robustly inhibits RANKL-induced NF-κB signaling.

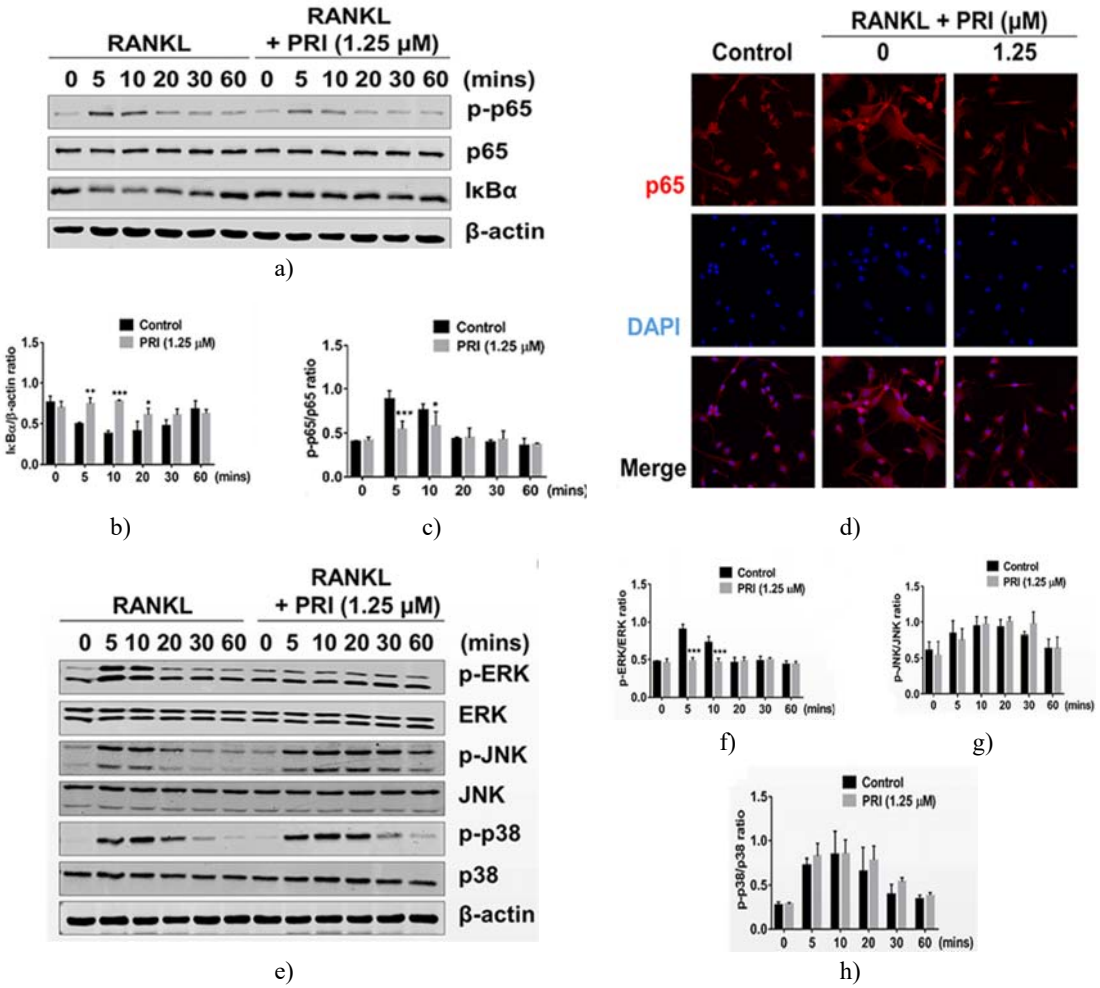

Figure 3. PRI Suppresses RANKL-Triggered NF-κB and ERK MAPK Pathways

(a) Immunoblot analysis showing early NF-κB activation in BMMs pretreated with 1.25 μM PRI for 1 hour and then stimulated with 50 ng/mL RANKL for varying times. Total and phosphorylated p65, as well as IκBα, were detected with specific antibodies; β-actin served as loading control.

(b, c) Quantification of protein band intensities for IκBα (normalized to β-actin) and p-p65 (normalized to total p65) using ImageJ.

(d) Confocal images illustrating nuclear translocation of p65 following RANKL treatment with or without PRI (magnification = 40×); nuclei were stained with DAPI.
(e) Western blots depicting the effects of PRI on the MAPK signaling cascade (ERK, JNK, p38) following RANKL stimulation.
(f–h) Densitometric analyses of phosphorylated ERK, JNK, and p38 relative to total protein levels. Data represent mean ± SD of three independent experiments; *p < 0.05, **p < 0.01, ***p < 0.001 vs RANKL only.

PRI selectively targets ERK signaling

Activation of MAPKs—including ERK, JNK, and p38—is crucial for the differentiation of BMMs into osteoclasts. Upon RANKL stimulation, phosphorylation of all three kinases was rapidly induced within 5 minutes **(Figures 3e–3h)**. ERK phosphorylation peaked at 10 minutes, while JNK and p38 remained phosphorylated for up to 20 minutes. Treatment with PRI specifically suppressed ERK phosphorylation but had little effect on p38. Interestingly, JNK phosphorylation appeared to be maintained longer in PRI-treated cells compared to controls **(Figures 3e and 3g)**. These results suggest that PRI selectively inhibits ERK activation while modulating JNK signaling during osteoclastogenesis.

PRI impairs NFATc1 expression and nuclear localization

NF-κB and MAPK signaling are critical for the induction of osteoclast-specific transcription factors, particularly c-Fos and NFATc1, which regulate genes required for osteoclast differentiation, fusion, and resorptive function [10, 19, 20] **(Figures 4a–4c)**. PRI treatment markedly reduced the RANKL-induced expression of both c-Fos and NFATc1 by day 3. Furthermore, PRI inhibited the translocation of NFATc1 into the nucleus **(Figure 4d)**, indicating a strong blockade of its transcriptional activity. Together, these data demonstrate that PRI disrupts early RANKL signaling, thereby preventing downstream activation of transcriptional programs necessary for osteoclast formation and function.

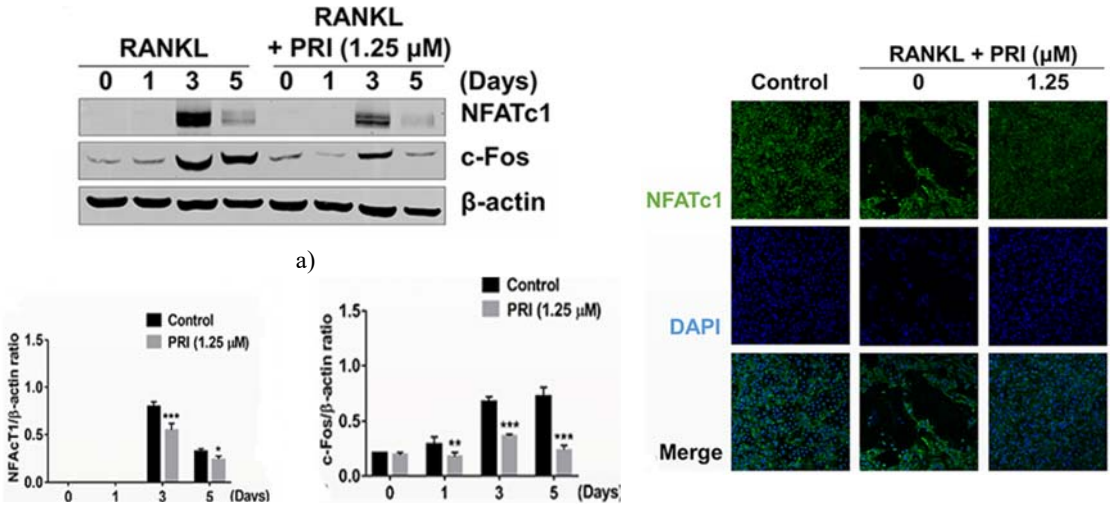

Figure 4. PRI Suppresses RANKL-Induced c-Fos and NFATc1 Expression

(a) Western blot analysis showing the effect of PRI on the expression of transcription factors c-Fos and NFATc1 in BMM-derived osteoclasts. Cells were co-treated with 50 ng/mL RANKL and 1.25 μM PRI for 0, 1, 3, and 4 days. β-actin served as a loading control.
(b, c) Quantitative densitometry of NFATc1 and c-Fos protein levels relative to β-actin, calculated using ImageJ.
(d) Confocal immunofluorescence illustrating the nuclear localization of NFATc1 following RANKL stimulation with or without PRI treatment (1.25 μM) (magnification = 20×). Nuclei were counterstained with DAPI. Data are presented as mean ± SD from at least three independent experiments; *p < 0.05, **p < 0.01, ***p < 0.001 vs RANKL-only controls.

PRI mitigates OVX-induced bone loss in mice

To examine whether the anti-osteoclastic and anti-resorptive effects of PRI observed in vitro translate to in vivo benefits, we employed a murine ovariectomy (OVX) model of post-menopausal bone loss. One week after OVX or sham surgery, mice were administered intraperitoneal injections of either saline or PRI (5 mg/kg) every other day for 6 weeks. High-resolution micro-CT imaging of excised tibiae revealed severe bone deterioration in saline-treated OVX mice compared to Sham controls **(Figure 5a)**. Morphometric quantification demonstrated a marked reduction in bone volume fraction (BV/TV), trabecular number (Tb.N), bone mineral density (BMD), and connectivity density (Conn.Dn), accompanied by an increase in trabecular separation (Tb.Sp) (**Figures 5b–5d and 5f–5g)**, consistent with osteoporotic bone loss.

In contrast, PRI-treated OVX mice displayed significantly preserved bone microarchitecture, with improved BV/TV, Tb.N, BMD, Conn.Dn, and decreased Tb.Sp compared to saline-treated OVX animals **(Figures 5a–5g)**. No significant changes in trabecular thickness (Tb.Th) were observed between groups **(Figure 5e)**. These findings indicate that PRI effectively protects against OVX-induced bone loss and preserves bone structural integrity in vivo.

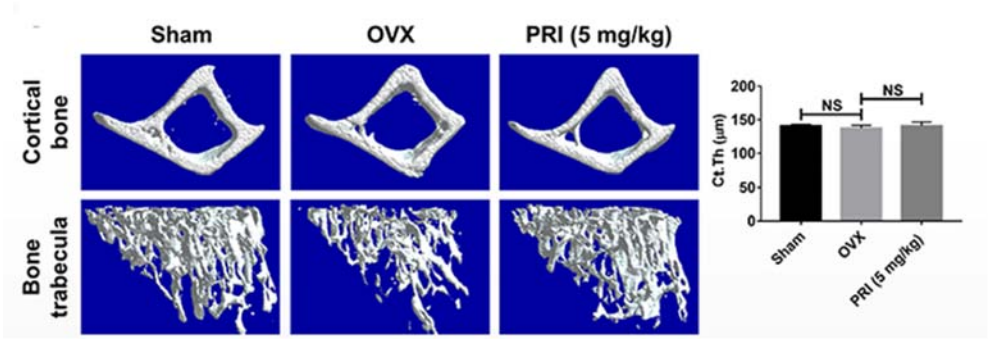

a)

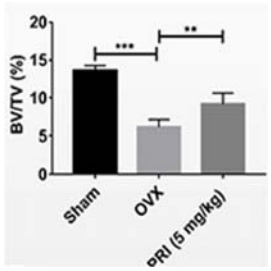

b)

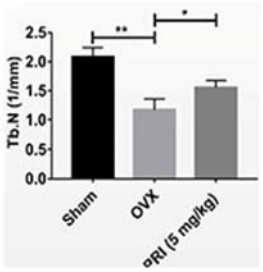

c)

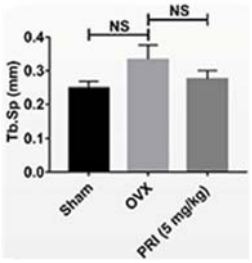

d)

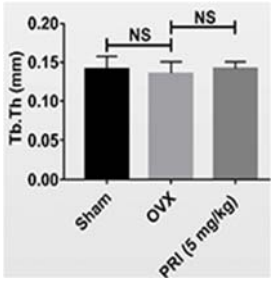

e)

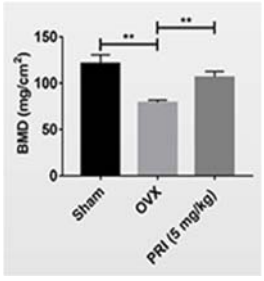

f)

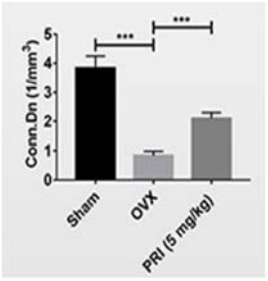

g)

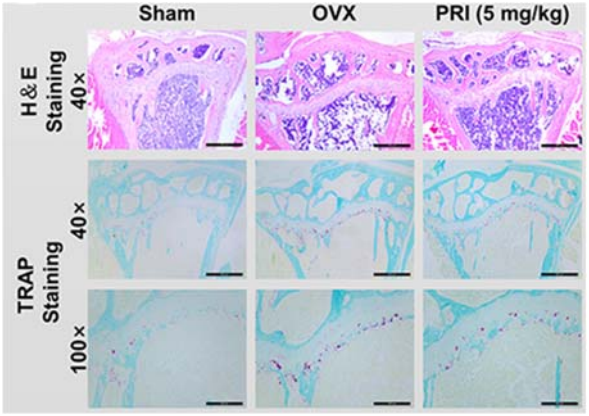

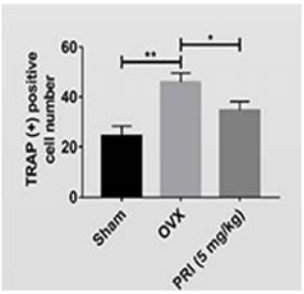

h) i)

Figure 5. PRI Attenuates OVX-Induced Bone Loss in Mice

(a) Three-dimensional micro-CT reconstructions of tibial trabecular and cortical bone from Sham (saline), OVX (saline), and OVX + PRI (5 mg/kg) mice.

(b–g) Quantitative bone morphometry showing BV/TV (%), trabecular number (Tb.N, mm^{-1}), trabecular separation (Tb.Sp, mm), trabecular thickness (Tb.Th, mm), bone mineral density (BMD, mg/cm^2), and connectivity density (Conn.Dn, $1/mm^3$).

(h) Representative histological sections stained with H&E and TRAP from tibiae of different groups.

(i) Quantification of TRAP-positive multinucleated osteoclasts in each group. Data are presented as mean ± SD, n = 8 per group; *p < 0.05, **p < 0.01, ***p < 0.001 versus control.

Histological evaluation corroborated the micro-CT findings, showing that PRI administration mitigated OVX-induced trabecular bone loss **(Figure 5h)**. TRAP staining further demonstrated a marked reduction in osteoclast numbers in PRI-treated OVX mice compared with untreated OVX controls **(Figures 5h–5i)**. Collectively, these results indicate that the in vitro anti-osteoclastic and anti-resorptive effects of PRI translate into significant protection against OVX-induced bone loss in vivo.

Results and Discussion

Bone homeostasis is maintained by the coordinated activities of osteoclasts, which mediate bone resorption, and osteoblasts, responsible for bone formation. This interplay ensures skeletal structural integrity. Dysregulation of this balance, particularly excessive osteoclast activity, underlies osteolytic disorders such as post-menopausal osteoporosis [21]. Current anti-resorptive therapies—including bisphosphonates, calcium supplementation, estrogen replacement, selective estrogen receptor modulators, and anti-RANKL antibodies—have demonstrated clinical efficacy [22]. However, these treatments are often associated with severe side effects, such as cardiovascular complications, nephrotoxicity, osteonecrosis of the jaw, atypical fractures, and increased tumor risk [4, 5, 23], limiting their long-term application. Therefore, the development of safer, effective alternatives remains a priority in osteoporosis management.

Our findings reveal that pristimerin (PRI), a natural triterpenoid from the Celastraceae and Hippocrateaceae families, inhibits osteoclast differentiation and bone resorption, protecting against OVX-induced bone loss. PRI has previously been reported to possess chemopreventive and chemotherapeutic effects [24], as well as anti-inflammatory, antioxidant, anti-arthritic, anti-malarial, antiviral, antibacterial, and anti-tumor activities [12, 14, 15, 25–28]. The present study expands the known biological effects of PRI by demonstrating its anti-osteoclastic and anti-resorptive potential.

Osteoclast differentiation is driven by the interaction of RANKL with its receptor RANK on monocyte/macrophage precursors, which recruits the adaptor protein TRAF6 to initiate downstream signaling cascades that promote cell fusion into multinucleated osteoclasts and activation of bone resorption [29]. Among these pathways, NF-κB and MAPK signaling (ERK, JNK, and p38) are crucial for early osteoclastogenesis. Activation of TRAF6 stimulates TAK1, which subsequently activates the IκB kinase (IKK) complex. IKK phosphorylates IκBα, triggering its ubiquitination and proteasomal degradation. This releases the p65/p50 NF-κB

heterodimers, allowing their phosphorylation, nuclear translocation, and initiation of transcriptional programs required for osteoclast differentiation [30]. NF-κB deficiency in double-knockout mice results in severe osteopetrosis due to impaired osteoclast formation [31].

Our biochemical analyses demonstrate that PRI effectively inhibits NF-κB activation by preventing IκBα degradation, p65 phosphorylation, nuclear translocation, and downstream transcriptional activity. These results are consistent with previous studies in murine macrophages [26] and multiple cancer cell types, including myeloma, fibrosarcoma, osteosarcoma, esophageal carcinoma, ovarian carcinoma, pancreatic cancer, and leukemia cells [15, 32–35].

Interestingly, Lu *et al*. reported that PRI can inhibit two critical steps in the NF-κB signaling cascade: the activation of IKK by TAK1 and the subsequent IKK-mediated phosphorylation of IκBα, the latter of which aligns with our observations. TAK1 also serves as an upstream MAP3K that triggers the three primary MAPK pathways—ERK, JNK, and p38—which together play essential roles in promoting osteoclast differentiation [36]. Studies using JNK1 or ERK1 knockout mice show that monocytic precursors lacking these kinases have diminished capacity to differentiate into osteoclasts [37, 38]. Beyond differentiation, ERK signaling contributes to osteoclast survival and maintenance of cell polarity during bone resorption [39], whereas p38 is primarily involved in osteoclast formation rather than resorptive activity [40].

Our findings reveal that PRI markedly suppresses ERK activation while leaving p38 unaffected. This ERK inhibition is consistent with prior reports linking PRI to pro-apoptotic effects [41]. Unexpectedly, PRI treatment prolonged RANKL-induced JNK activation. Previous studies have demonstrated that PRI can induce apoptosis and autophagy via ROS generation, which in turn activates the ASK1/JNK pathway in human breast cancer and chronic myeloid leukemia cells [42]. Therefore, the sustained JNK phosphorylation observed here may be attributed to ROS-mediated ASK1/JNK activation, though further investigation is warranted.

Early NF-κB and MAPK activation coordinates the induction of transcription factors c-Fos and NFATc1, both essential for osteoclastogenesis [9]. Loss of c-Fos or NFATc1 abolishes osteoclast formation, resulting in severe osteopetrosis in mice [10]. Notably, overexpression of NFATc1 can rescue osteoclast defects in c-Fos- or NF-κB-deficient models, highlighting NFATc1 as a critical distal regulator of osteoclast differentiation [43]. NFATc1 activation is initially triggered by early RANKL signaling and is subsequently sustained via Ca^{2+} oscillation-mediated auto-amplification [44]. Once activated, NFATc1 translocates to the nucleus and cooperates with other transcription factors to drive expression of osteoclast-specific genes such as Dc-stamp, Trap/Acp5, Mmp-9, and Ctsk [11]. In line with PRI-mediated inhibition of NF-κB and ERK pathways, both c-Fos and NFATc1 induction and NFATc1 nuclear localization were significantly suppressed. Correspondingly, transcription of downstream osteoclast markers, including Trap/Acp5, Dc-stamp, Mmp-9, and Ctsk, was markedly reduced following PRI treatment.

Overall, our data indicate that PRI exerts anti-osteoclastic effects by restraining RANKL-mediated activation of ERK MAPK and NF-κB signaling, thereby preventing downstream activation of c-Fos and NFATc1, which are essential for osteoclast differentiation, fusion, and bone resorption. Importantly, the in vitro anti-resorptive and anti-osteoclastic effects of PRI translated to in vivo protection, as PRI administration mitigated estrogen-deficiency–induced bone loss in OVX mice. Morphometric analyses showed significant improvements in bone volume and trabecular architecture, while histological evaluation revealed a reduction in osteoclast numbers and activity. Collectively, these findings provide strong evidence supporting PRI as a potential therapeutic agent for osteoclast-mediated osteolytic diseases.

Acknowledgments: This work is supported by the Natural Science Foundation of China (No.81770254, No.81970236) and Natural Science Foundation of Guangxi Province (2018GXNSFAA050092).

Conflict of Interest: None

Financial Support: None

Ethics Statement: This work fully considered and protected the rights and interests of the study objects. The use of animals in experiments was approved by the ethics Committee of Guangxi medical university (SYXK 2020-0004). All experimental procedures were performed in conformity with institutional guidelines for the care and

use of laboratory animals Guangxi medical university, China. This project meets the criteria of the Ethical Review Committee.

References

1. Su N, Yang J, Xie Y, Du X, Lu X, Huang Y, et al. Bone function, dysfunction and its role in diseases including critical illness. Int J Biol Sci. 2019;15(4):776-87. doi:10.7150/ijbs.27063
2. Cao X. Targeting osteoclast-osteoblast communication. Nat Med. 2011;17(11):1344-6. doi:10.1038/nm.2499
3. Compston JE, McClung MR, Leslie WD. Osteoporosis. Lancet. 2019;393(10169):364-76. doi:10.1016/S0140-6736(18)32112-3
4. Milat F, Ebeling PR. Osteoporosis treatment: a missed opportunity. Med J Aust. 2016;205(4):185-90. doi:10.5694/mja16.00568
5. Reid IR. Efficacy, effectiveness and side effects of medications used to prevent fractures. J Intern Med. 2015;277(6):690-706. doi:10.1111/joim.12339
6. Feng X. RANKing intracellular signaling in osteoclasts. IUBMB Life. 2005;57(6):389-95. doi:10.1080/15216540500137669
7. Chen R, Liu G, Sun X, Cao H, Huang X, Chen Y, et al. Chitosan derived nitrogen-doped carbon dots suppress osteoclastic osteolysis via downregulating ROS. Nanoscale. 2020;12(30):16229-44. doi:10.1039/D0NR02848G
8. Nakashima T, Takayanagi H. New regulation mechanisms of osteoclast differentiation. Ann N Y Acad Sci. 2011;1240:E13-8. doi:10.1111/j.1749-6632.2011.06373.x
9. Wagner EF. Bone development and inflammatory disease is regulated by AP-1 (Fos/Jun). Ann Rheum Dis. 2010;69 Suppl 1:i86-8. doi:10.1136/ard.2009.119396
10. Takayanagi H, Kim S, Koga T, Nishina H, Isshiki M, Yoshida H, et al. Induction and activation of the transcription factor NFATc1 (NFAT2) integrate RANKL signaling in terminal differentiation of osteoclasts. Dev Cell. 2002;3(6):889-901. doi:10.1016/S1534-5807(02)00369-6
11. Fretz JA, Shevde NK, Singh S, Darnay BG, Pike JW. Receptor activator of nuclear factor-kappaB ligand-induced nuclear factor of activated T cells (C1) autoregulates its own expression in osteoclasts and mediates the up-regulation of tartrate-resistant acid phosphatase. Mol Endocrinol. 2008;22(3):737-50. doi:10.1210/me.2007-0333
12. Sun Y, Gao LL, Tang MY, Feng BM, Pei YH, Yasukawa K. Triterpenoids from Euphorbia maculata and their anti-inflammatory effects. Molecules. 2018;23(9):2112. doi:10.3390/molecules23092112
13. Buffa Filho W, Corsino J, da Silva Bolzani V, Furlan M, Pereira AM, França SC. Quantitative determination for cytotoxic Friedo-nor-oleanane derivatives from five morphological types of Maytenus ilicifolia (Celastraceae) by reverse-phase high-performance liquid chromatography. Phytochem Anal. 2002;13(2):75-8. doi:10.1002/pca.626
14. Li JJ, Yan YY, Sun HM, Liu Y, Su CY, Chen HB, et al. Anti-cancer effects of pristimerin and the mechanisms: a critical review. Front Pharmacol. 2019;10:746. doi:10.3389/fphar.2019.00746
15. Tong L, Nanjundaiah SM, Venkatesha SH, Astry B, Yu H, Moudgil KD. Pristimerin, a naturally occurring triterpenoid, protects against autoimmune arthritis by modulating the cellular and soluble immune mediators of inflammation and tissue damage. Clin Immunol. 2014;155(2):220-30. doi:10.1016/j.clim.2014.09.014
16. Xiao Y, Li K, Wang Z, Fu F, Shao S, Song X, et al. Pectolinarigenin prevents bone loss in ovariectomized mice and inhibits RANKL-induced osteoclastogenesis via blocking activation of MAPK and NFATc1 signaling. J Cell Physiol. 2019;234(8):13959-68. doi:10.1002/jcp.28079
17. Jurdic P, Saltel F, Chabadel A, Destaing O. Podosome and sealing zone: specificity of the osteoclast model. Eur J Cell Biol. 2006;85(3-4):195-202. doi:10.1016/j.ejcb.2005.09.008
18. Jacobs MD, Harrison SC. Structure of an IκBα/NF-κB complex. Cell. 1998;95(6):749-58. doi:10.1016/S0092-8674(00)81698-0
19. Arai A, Mizoguchi T, Harada S, Kobayashi Y, Nakamichi Y, Yasuda H, et al. Fos plays an essential role in the upregulation of RANK expression in osteoclast precursors within the bone microenvironment. J Cell Sci. 2012;125(Pt 12):2910-7. doi:10.1242/jcs.099986

20. Balkan W, Martinez AF, Fernandez I, Rodriguez MA, Pang M, Troen BR. Identification of NFAT binding sites that mediate stimulation of cathepsin K promoter activity by RANK ligand. Gene. 2009;446(2):90-8. doi:10.1016/j.gene.2009.06.013
21. D'Amelio P, Grimaldi A, Di Bella S, Brianza SZ, Cristofaro MA, Tamone C, et al. Estrogen deficiency increases osteoclastogenesis up-regulating T cells activity: a key mechanism in osteoporosis. Bone. 2008;43(1):92-100. doi:10.1016/j.bone.2008.02.017
22. Brommage R. New targets and emergent therapies for osteoporosis. Handb Exp Pharmacol. 2020;262:451-73. doi:10.1007/164_2019_329
23. Zhang J, Saag KG, Curtis JR. Long-term safety concerns of antiresorptive therapy. Rheum Dis Clin North Am. 2011;37(3):387-400, vi. doi:10.1016/j.rdc.2011.08.001
24. Niampoka C, Suttisri R, Bavovada R, Takayama H, Aimi N. Potentially cytotoxic triterpenoids from the root bark of Siphonodon celastrineus Griff. Arch Pharm Res. 2005;28(5):546-9. doi:10.1007/BF02977756
25. Costa PM, Ferreira PM, da Silva Bolzani V, Furlan M, dos Santos VA, Corsino J, et al. Antiproliferative activity of pristimerin isolated from Maytenus ilicifolia (Celastraceae) in human HL-60 cells. Toxicol In Vitro. 2008;22(4):854-63. doi:10.1016/j.tiv.2008.01.003
26. Dirsch VM, Kiemer AK, Wagner H, Vollmar AM. The triterpenoid quinonemethide pristimerin inhibits induction of inducible nitric oxide synthase in murine macrophages. Eur J Pharmacol. 1997;336(2-3):211-7. doi:10.1016/S0014-2999(97)01245-4
27. Huang S, He P, Peng X, Li J, Xu D, Tang Y. Pristimerin inhibits prostate cancer bone metastasis by targeting PC-3 stem cell characteristics and VEGF-induced vasculogenesis of BM-EPCs. Cell Physiol Biochem. 2015;37(1):253-68. doi:10.1159/000430350
28. Yan YY, Bai JP, Xie Y, Yu JZ, Ma CG. The triterpenoid pristimerin induces U87 glioma cell apoptosis through reactive oxygen species-mediated mitochondrial dysfunction. Oncol Lett. 2013;5(1):242-8. doi:10.3892/ol.2012.982
29. Kobayashi N, Kadono Y, Naito A, Matsumoto K, Yamamoto T, Tanaka S, et al. Segregation of TRAF6-mediated signaling pathways clarifies its role in osteoclastogenesis. EMBO J. 2001;20(6):1271-80. doi:10.1093/emboj/20.6.1271
30. Ruocco MG, Maeda S, Park JM, Lawrence T, Hsu LC, Cao Y, et al. IκB kinase (IKK)β, but not IKKα, is a critical mediator of osteoclast survival and is required for inflammation-induced bone loss. J Exp Med. 2005;201(10):1677-87. doi:10.1084/jem.20042081
31. Iotsova V, Caamaño J, Loy J, Yang Y, Lewin A, Bravo R. Osteopetrosis in mice lacking NF-κB1 and NF-κB2. Nat Med. 1997;3(11):1285-9. doi:10.1038/nm1197-1285
32. Tiedemann RE, Schmidt J, Keats JJ, Schop RF, Kortuem KM, Storz P, et al. Identification of a potent natural triterpenoid inhibitor of proteosome chymotrypsin-like activity and NF-κB with antimyeloma activity in vitro and in vivo. Blood. 2009;113(17):4027-37. doi:10.1182/blood-2008-09-179796
33. Wang Y, Zhou Y, Zhou H, Jia W, Jin Y, Li J, et al. Pristimerin causes G1 arrest, induces apoptosis, and enhances the chemosensitivity to gemcitabine in pancreatic cancer cells. PLoS One. 2012;7(8):e43826. doi:10.1371/journal.pone.0043826
34. Gao X, Liu Y, Deeb D, Arbab AS, Gautam SC. Anticancer activity of pristimerin in ovarian carcinoma cells is mediated through the inhibition of prosurvival Akt/NF-κB/mTOR signaling. J Exp Ther Oncol. 2014;10(4):275-83.
35. Tu Y, Tan F, Zhou J, Pan J. Pristimerin targeting NF-κB pathway inhibits proliferation, migration, and invasion in esophageal squamous cell carcinoma cells. Cell Biochem Funct. 2018;36(4):228-40. doi:10.1002/cbf.3335
36. Mizukami J, Takaesu G, Akatsuka H, Sakurai H, Ninomiya-Tsuji J, Matsumoto K, et al. Receptor activator of NF-κB ligand (RANKL) activates TAK1 mitogen-activated protein kinase kinase kinase through a signaling complex containing RANK, TAB2, and TRAF6. Mol Cell Biol. 2002;22(4):992-1000. doi:10.1128/MCB.22.4.992-1000.2002
37. He Y, Staser K, Rhodes SD, Liu Y, Wu X, Park SJ, et al. Erk1 positively regulates osteoclast differentiation and bone resorptive activity. PLoS One. 2011;6(9):e24780. doi:10.1371/journal.pone.0024780

38. David JP, Sabapathy K, Hoffmann O, Idarraga MH, Wagner EF. JNK1 modulates osteoclastogenesis through both c-Jun phosphorylation-dependent and -independent mechanisms. J Cell Sci. 2002;115(Pt 22):4317-25. doi:10.1242/jcs.00082
39. Nakamura H, Hirata A, Tsuji T, Yamamoto T. Role of osteoclast extracellular signal-regulated kinase (ERK) in cell survival and maintenance of cell polarity. J Bone Miner Res. 2003;18(7):1198-205. doi:10.1359/jbmr.2003.18.7.1198
40. Lee K, Chung YH, Ahn H, Kim H, Rho J, Jeong D. Selective regulation of MAPK signaling mediates RANKL-dependent osteoclast differentiation. Int J Biol Sci. 2016;12(2):235-45. doi:10.7150/ijbs.13814
41. Hayashi D, Shirai T, Terauchi R, Tsuchida S, Mizoshiri N, Mori Y, et al. Pristimerin inhibits the proliferation of HT1080 fibrosarcoma cells by inducing apoptosis. Oncol Lett. 2020;19(4):2963-70.
42. Zhao Q, Liu Y, Zhong J, Bi Y, Liu Y, Ren Z, et al. Pristimerin induces apoptosis and autophagy via activation of ROS/ASK1/JNK pathway in human breast cancer in vitro and in vivo. Cell Death Discov. 2019;5:125. doi:10.1038/s41420-019-0208-0
43. Matsuo K, Galson DL, Zhao C, Peng L, Laplace C, Wang KZ, et al. Nuclear factor of activated T-cells (NFAT) rescues osteoclastogenesis in precursors lacking c-Fos. J Biol Chem. 2004;279(25):26475-80. doi:10.1074/jbc.M313973200
44. Park YJ, Yoo SA, Kim M, Kim WU. The role of calcium-calcineurin-NFAT signaling pathway in health and autoimmune diseases. Front Immunol. 2020;11:195. doi:10.3389/fimmu.2020.00195